Environmental Science Processes & Impacts

ROYAL SOCIETY OF CHEMISTRY

PAPER

View Article Online
View Journal | View Issue

Cite this: *Environ. Sci.: Processes Impacts*, 2023, **25**, 2102

Feedstock nitrogen content mediates maximum possible Pb sorption capacity of biochars†

Chinonso Ogbuagu, Steve Robinson and Tom Sizmur *

The use of biochar for the adsorption of contaminants from soil and water has received considerable interest due to biochar's high surface area, negative charge, and resistance to degradation. However, a knowledge gap still exists concerning the optimum selection of feedstocks and pyrolysis temperatures to maximise sorption capacity for metals. In this study, biochars were produced from 4 different feedstock materials (hay, wheat straw, coco coir, and pine bark) at 10 pyrolysis temperatures ranging from 300 °C to 750 °C, at 50 °C intervals. Batch sorption experiments were conducted to determine the maximum Pb sorption capacity for each biochar using the Langmuir model. The sorption isotherms fit the Langmuir model well (generally R^2 > 0.7). The Langmuir maximum sorption capacity increased with an increase in pyrolysis temperature, according to a sigmoidal relationship. A sigmoidal model was fit to the data to derive the theoretical maximum possible sorption capacity obtainable from a feedstock. We observed a positive correlation between the nitrogen content of the feedstock and the theoretical maximum possible sorption capacity obtainable from the feedstock. This relationship highlights the importance of nitrogen content in feedstock to create biochars with a high Pb sorption capacity. It is possible that cation–π interactions with heterocyclic N structures are the primary mechanism for the sorption of Pb to these biochars, and this warrants further investigation.

Received 6th June 2023
Accepted 24th October 2023

DOI: 10.1039/d3em00246b

rsc.li/espi

Environmental significance

Currently, biochars are made from available feedstocks without full knowledge of what the resultant biochar properties will be and how effective the biochars will be for Pb sorption. The utility of other available feedstocks is unknown without arbitrary experimentation. We observed a positive correlation between the nitrogen content of feedstocks and the theoretical maximum possible sorption capacity of biochars made from the feedstocks. This relationship highlights the role played by heterocyclic N structures in the sorption of Pb to biochar and the importance of feedstock nitrogen content to create biochars with a high Pb sorption capacity. We report a formula that enables remediation engineers to select biochar feedstocks optimal for Pb sorption based on the nitrogen content of the feedstock.

Introduction

Pollution of water and soil with lead (Pb) is a global problem arising from anthropogenic activities such as smelting, mining, agricultural activities, and industrialization.[1] Pb is a very abundant contaminant, which may cause adverse effects in the environment.[2] These adverse effects have led to the banning of some Pb-containing products such as leaded fuel and Pb pigments. Studies have shown negative impacts of Pb contamination on soil microorganisms, soil quality, animals, and humans.[3,4] The need to remediate Pb contaminated soil and water is vital for environmental quality and human health. Therefore, we need to develop sustainable, low-cost remediation methods.

Biochar is a carbonaceous material obtained from the pyrolysis of organic feedstocks under anaerobic conditions.[5,6] Biochar in recent years has received considerable attention due to its low cost and effective capability of removing heavy metals from solution[7] and reducing their mobility and bioavailability in soils.[8] Biochars are mainly made from organic wastes, such as rice husks,[9] pistachio shells,[7] and forest residues,[10] which are cheap,[11] and readily available,[12] and transforms linear material flows into cyclic loops.[13] Studies have shown how biochar application to soil and water is able to reduce the availability of Pb. For example, Lu, Zhang[14] observed that sludge biochar pyrolyzed at 550 °C had a maximum sorption capacity of 30.9 mg g^{-1} for Pb. In another study, Ahmad, Gao,[15] observed that the maximum sorption capacity for Pb using banana peel biochar and cauliflower biochar pyrolyzed at 600 °C were 247 mg g^{-1} and 178 mg g^{-1}, respectively. Liu, Huang[16] used multiple feedstocks from rice straw, rice husk, and sawdust pyrolyzed at 400 °C, 500 °C, and 600 °C and observed maximum sorption

Soil Research Centre, Department of Geography and Environmental Science, University of Reading, Reading, UK. E-mail: t.sizmur@reading.ac.uk

† Electronic supplementary information (ESI) available. See DOI: https://doi.org/10.1039/d3em00246b

capacities of 128 mg g^{-1} for rice straw biochar pyrolyzed at 550 °C, 30.4 mg g^{-1} for rice husk biochar pyrolyzed at 600 °C, and 24.1 mg g^{-1} for sawdust biochar pyrolyzed at 600 °C. In another study, biochar derived from cotton stalk pyrolyzed at 550 °C was observed to have a maximum Pb sorption capacity of 147 mg g^{-1}.[17]

The observations from literature outlined above shows that the differences in the maximum sorption capacities of Pb are influenced by both the feedstock type and the pyrolysis temperature. Together these factors influence the biochar's physiochemical properties; such as cation exchange capacity, surface area (micropores and mesopores), elemental composition, abundance of functional groups (carboxyl, hydroxyl, aromatic, and amino groups), and pH. For example, woody biomass feedstocks are characterised with high lignin, hemicellulose, and cellulose content compared to grass or herbaceous feedstocks.[18,19] These feedstocks contrast with manures, composts, and sludges, which are high in N content.[20] Low pyrolysis temperatures (200 °C to 450 °C) create biochars with low pH, low surface area, and a greater abundance of oxygenated functional groups (carboxyl and hydroxyl).[21] The sorption of Pb to biochars produced at low pyrolysis temperature has been attributed to specific adsorption due to complexation and cation exchange with oxygenated functional groups.[22] At high pyrolysis temperature there is increased carbonisation of the biochar, an increase in pH, an increase in the surface area, and an increase in the abundance of aromatic functional groups.[23] The formation of aromatic structures results in non-specific adsorption of Pb due to cation–π interactions.[8]

All the above-mentioned studies have shown that biochar can adsorb and reduce the availability of Pb in soil and solution. However, there is still limited mechanistic research explaining how feedstock properties influence the biochar properties, and how these biochar properties, in turn, influence the sorption capacity. For this reason, arbitrary experimentation is required to trial different feedstocks at different pyrolysis temperatures to identify a biochar that has an optimal sorption capacity. It would save time and resources if the sorption capacity of a biochar could be predicted, based on the feedstock properties, without any prior experimentation.

In this study, we examined how pyrolysis temperature and feedstock properties of four feedstocks influenced the ability of a biochar to adsorb Pb from solution. We hypothesised that feedstock C/N ratio would influence biochar sorption capacity, based upon a prior relationship between feedstock C/N ratio and Cu and Zn sorption by biochars reported by Rodríguez-Vila, Selwyn-Smith.[24]

Materials and methods

Biochar production

Biochars were produced from four different feedstock materials: hay, wheat straw, coco coir, and pine bark. The coco coir and hay were bought from a hardware store (B&Q) and a home store (B&M), respectively. The pine bark and wheat straw were obtained from Park Farm, Oakley, and the University of Reading's farm at Sonning, respectively. The C/N ratios of the feedstocks ranged between 534 and 37 and are given in Table 1.

Table 1 Carbon content (C%), nitrogen content (N%), and C/N ratio of hay, wheat straw, coco coir, and pine bark feedstocks used to make biochar

Feedstock	N (%)	C (%)	C/N ratio
Hay	1.11	41.4	37.3
Wheat straw	0.73	44.2	60.7
Coco coir	0.44	44.2	101
Pine bark	0.09	45.9	534

Prior to biochar production, the feedstock materials were air dried for 24 hours to reduce the moisture content. The feedstock materials were packed in steel containers (diameter 10 cm, height 18.2 cm) with a small hole cut into the lid to avoid pressure build up. The containers were heated to the desired temperature for one hour using a Gallenkamp muffle furnace to pyrolyse the feedstocks and then allowed to cool overnight before the biochar was removed. Biochars were made from each of the four feedstocks at 300 °C, 350 °C, 400 °C, 450 °C, 500 °C, 550 °C, 600 °C, 650 °C, 700 °C, and 750 °C, resulting in a total of 40 different biochars. The biochars were each ground to a fine powder using a TEMA T100ACH Laboratory Disc Mill.

Biochar and feedstock characterisation

The biochar yield was determined by measuring the weight of feedstock before pyrolysis and weight of biochar produced after pyrolysis. Biochar pH was determined in triplicate by shaking 1 g of biochar with 20 mL of ultra-pure water for 30 minutes and measuring the pH (HANNA HI 9812-5) of the biochar/water slurry. Approximately 4 mg of each ground biochar and feedstock sample was weighed into tin cups using a five-place balance and analysed for total carbon and nitrogen content by dry combustion using a Thermo Scientific Flash 2000 Organic Elemental Analyser, calibrated with 1 and 3 mg samples of an aspartic acid. Biochars and feedstocks were digested in nitric acid prior to determination of Ca, Mg, K, P, S, Na, Cu, Pb, Mn, Zn, Al, and Fe by ICP-OES (Inductively Coupled Plasma Optical Emission Spectroscopy). Briefly, 0.5 g of each biochar or feedstock was weighed into a 100 mL glass Kjeldahl digestion tube. 10 mL of concentrated nitric acid was added and tubes left overnight with a glass bubble covering the opening. Tubes were then heated to 60 °C and held for three hours before ramping up to 110 °C and holding for a further six hours. Digestates were filtered with Whatman 540 filter papers and diluted prior to ICP-OES analysis. The full dataset containing biochar chemical properties can be found at ref. 25. Fourier Transform Infrared (FTIR) spectra were obtained for all 40 biochar samples and the 4 feedstock materials using a PerkinElmer Spectrum 100 FTIR spectrometer equipped with a universal attenuated total reflectance (ATR) sampling accessory. The samples were scanned in the range from 4000 cm^{-1} to 650 cm^{-1} and a resolution of 4 cm^{-1} with 32 scans per sample. Peaks were assigned to

functional groups as described in the ESI and summarised in Table S-1.†

Batch sorption experiment

Pb batch adsorption isotherms were carried out for each of the 40 biochars using five Pb solutions (100, 200, 500, 1000, and 5000 mg Pb per L) prepared by serial dilution of a 5000 mg per L stock solution of lead nitrate made by dissolving analytical grade $Pb(NO_3)_2$ in >18.2 MΩ cm water. Milled biochar (1 g ± 0.05 g) was weighed into a 50 polypropylene mL centrifuge tube and 30 mL of Pb solution was added to each sample. Samples were placed in a rotary end-over-end shaker at 20 inversions per minute, at a controlled temperature of 20 °C for 24 hours for to ensure equilibrium between biochar surfaces and the Pb in solution. After 24 hours, samples were removed from the shaker and the pH was measured and recorded (Table S-2†). Samples were then centrifuged at 3600 rpm for 15 minutes to separate the biochar particles from solution using a Mistral 3000i centrifuge. The supernatant was filtered through a Whatman no. 5 filter paper. Further filtration was carried out using a 0.2 μm cellulose membrane syringe filter. Samples were then diluted and acidified using concentrated nitric acid (HNO_3) and analysed for Pb concentration using an ICP-OES.

Sorption isotherm model fitting

The quantity of Pb sorbed to each of the biochars was calculated using eqn (1):

$$C_s = \frac{(C_i - C_{aq}) \times V}{S_m} \quad (1)$$

where C_s is the Pb concentration on biochar (mg g^{-1}), C_i is the initial solution Pb concentration (mg L^{-1}), C_{aq} is the final solution Pb concentration (mg L^{-1}), V is the solution volume (L), and S_m is the mass of biochar (g).

The Langmuir sorption isotherm was then fit to the sorption data using eqn (2).

$$\frac{C_s}{C_{aq}} = \frac{bC_{sm}}{1 + C_{aq}b} \quad (2)$$

where C_s is the Pb concentration on biochar (mg g^{-1}), C_{aq} is the final solution Pb concentration (mg L^{-1}), b is the Langmuir binding constant and C_{sm} is the maximum sorption capacity of Pb on the biochar (mg g^{-1}).

The relationship between the maximum sorption capacity (C_{sm}), derived from by the Langmuir fits, and the pyrolysis temperature of the biochar was fit to a modified version of the sigmoidal model proposed by Rodríguez-Vila, Selwyn-Smith,[24] using eqn (3).

$$C_{sm} = x + \left(m\frac{PT^n}{PT^n + K^n}\right) \quad (3)$$

where x is the C_{sm} value for the biochar pyrolyzed at 300 °C, PT is the pyrolysis temperature, and m, k, and n are constants. $m + x$ is the maximum possible C_{sm} at the optimum pyrolysis temperature, k is the pyrolysis temperature at which $C_{sm} = m/2$, and n dictates the shape of the curve.

Quality control

All vessels and experimental equipment used for sorption isotherms were acid-washed. Blank samples with no biochar were used to detect contamination which may have occurred during sample handling, preparation, and analysis. Within each batch of sorption isotherms, a duplicate of the 450 °C biochar (but not the other biochars) was ran to quantify the precision of an isotherm. The calculated average relative standard deviation (% RSD) for each of the Pb solutions (100, 200, 500, 1000, and 5000 mg Pb per L) were 4.1%, 16.7%, 4.5%, 2.6% and 8.6% respectively.

One blank (empty cup) and one in-house reference material were included in each batch for analysis of C and N by dry combustion. We obtained a recovery of 99% ± 10% ($n = 3$) for carbon and 103% ± 10% for nitrogen ($n = 3$). The in-house reference material is traceable to certified reference materials AR4016, Alpha Resources (certified for carbon) and GBW07412, State Bureau of Technical Supervision, China (certified for nitrogen).

Each batch of acid digestions included two blanks and one sample of an in-house hay reference material, traceable to NCS DC 73349 Bush Branches and Leaves. We obtained a recovery of 81%, 93%, 102%, 89%, 90%, 96%, 86%, 109%, 88%, 93%, 88%, 101% for Al, Ca, Cu, Fe, K, Mg, Mn, Na, P, Pb, S and Zn, respectively.

Statistical analysis

Microsoft Excel Solver was used to fit experimental data to non-linear models. Minitab version 21 was used to fit regression models to quantify the relationship between biochar feedstock properties and the biochar maximum possible Pb sorption capacity.

Results

Most of the data fit the Langmuir model well (typically with $R^2 > 0.7$) (Table 2 and Fig. S-1–S-4†). For all four feedstocks, the maximum sorption capacity (C_{sm}) derived by the Langmuir equation increased as pyrolysis temperature increased from 300 °C to 750 °C (Table 2). The maximum Pb sorption capacities (C_{sm}) for biochars pyrolyzed at 750 °C was highest for hay (172 mg g^{-1}), followed by wheat straw, (164 mg g^{-1}), coco coir (139 mg g^{-1}), and then pine bark at (39 mg g^{-1}).

To characterise the relationship between the pyrolysis temperature and the maximum sorption capacity (C_{sm}) determined by the Langmuir isotherm model, the data was fit to a modified version of the sigmoidal model used by Rodríguez-Vila, Selwyn-Smith[24] eqn (3). We observed a clear sigmoidal relationship between maximum sorption capacity (C_{sm}) and pyrolysis temperature (Fig. 1). The constants derived from the fitted equation include m, which, when combined with x, is the maximum possible sorption capacity at the optimum pyrolysis temperature. $m + x$ was 198 mg g^{-1}, 167 mg g^{-1}, 125 mg g^{-1}, and 51.5 mg g^{-1} for hay, wheat straw, coco coir, and pine bark biochar, respectively (Table 3).

Table 2 Langmuir isotherm maximum sorption capacity (C_{sm} mg g^{-1}) and goodness of fit (R^2) for Pb sorption onto biochars pyrolyzed from hay, coco coir, pine bark, and wheat straw at 300 °C, 350 °C, 400 °C, 450 °C, 500 °C, 550 °C, 600 °C, 650 °C, 700 °C, and 750 °C

	Hay		Wheat straw		Coco coir		Pine bark	
Pyrolysis temperature (°C)	C_{sm} (mg g^{-1})	R^2	C_{sm} (mg g^{-1})	R^2	C_{sm} (mg g^{-1})	R^2	C_{sm} (mg g^{-1})	R^2
300	16.1	0.41	47.9	0.71	59.2	0.96	5.04	0.72
350	38.0	0.71	71.9	0.93	59.5	0.47	5.76	0.5
400	74.6	0.9	86.2	0.2	64.5	0.59	6.52	0.49
450	80.6	0.94	101	0.61	97.1	0.82	7.47	0.9
500	106	0.96	137	0.84	108	0.98	8.54	0.5
550	104	0.98	133	0.6	135	0.96	9.56	0.64
600	125	0.98	143	0.73	112	1	16.3	0.92
650	149	0.99	164	0.3	127	0.99	20.5	0.92
700	149	0.98	159	0.99	114	1	33.0	0.9
750	172	0.99	164	0.99	139	0.99	38.8	0.9

Regression analysis conducted between the parameters derived from the sigmoidal model (Table 3) and the biochar feedstock properties (Table S-3†) for each biochar feedstock revealed a strong and statistically significant relationship ($R^2 = 0.954$, $p < 0.05$) between $m + x$, the maximum possible Langmuir C_{sm} (maximum sorption capacity) at the optimum pyrolysis temperature, and nitrogen content (% N) of the biochar feedstock (Fig. 2). Feedstocks with a higher % N content had a higher maximum possible sorption capacity. There were no statistically significant relationships observed between maximum possible Pb sorption capacity and any of the other feedstock chemical properties analysed (Table S-4†). The

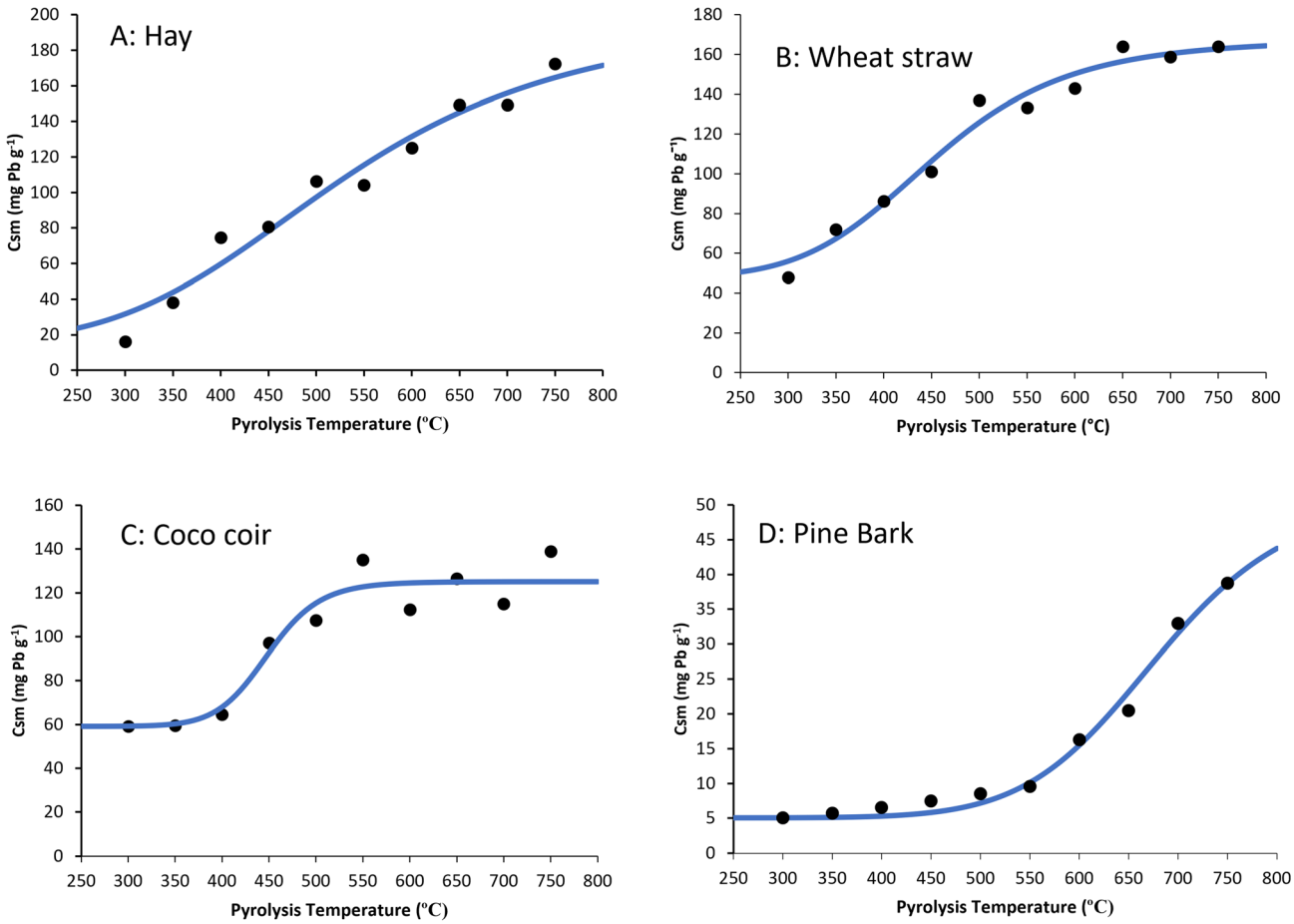

Fig. 1 Relationship between Pb sorption capacity and biochar pyrolysis temperature. Pb maximum sorption capacity (C_{sm}) of hay (A), wheat straw (B), coco coir (C), and pine bark (D) biochars plotted against pyrolysis temperature and fitted to a sigmoidal model that quantifies the relationship.

Table 3 Constants derived from fitting the relationship between maximum Pb sorption capacity (C_{sm}) and biochar pyrolysis temperature using eqn (3) for hay, wheat straw, coco coir, and pine bark biochars pyrolyzed between 300 °C and 750 °C[a]

Feedstock	x (mg g^{-1})	K (°C)	m (mg g^{-1})	n	$m + x$ (mg g^{-1})
Hay	16.1	527	182	4.19	198
Wheat straw	47.8	453	120	6.35	167
Coco coir	59.2	449	66	16.2	125
Pine bark	5	680	46.5	9.89	51.5

[a] $x = C_{sm}$ at 300 °C, $m + x$ is the maximum possible C_{sm} at the optimum pyrolysis temperature, k is the pyrolysis temperature at which $C_{sm} = m/2$, and n dictates the shape of the curve.

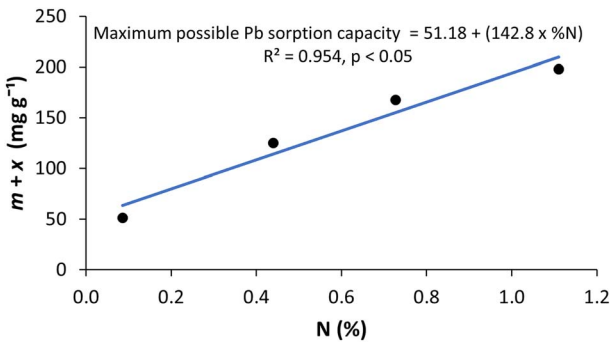

Fig. 2 Relationship between $m + x$ (the maximum possible Pb sorption capacity at the optimum pyrolysis temperature) and % N of the biochar feedstock.

relationship between feedstock % N content and maximum possible Pb sorption capacity is represented by eqn (4), which could be used to predict the maximum possible Pb sorption capacity of a biochar based on the N content of its feedstock.

$$m + x = 51.18 + (142.8 \times N) \quad (4)$$

where $m + x$ is the maximum possible Pb sorption capacity of the biochar (mg g^{-1}), and N is the percentage nitrogen content of the feedstock, measured by dry combustion.

It is clear from the FTIR spectra (Fig. S-5†) that the feedstocks contained more functional groups than the biochars. For example, the peak at 1160 cm^{-1}, which was attributed to C–O–C ester groups in cellulose and hemicellulose, is much more pronounced in the feedstock that in the biochars. As pyrolysis temperature increased, the size of most peaks declined and peaks were barely visible in the spectra of the biochars pyrolyzed at 750 °C.

Discussion

The biochars made from hay and wheat straw pyrolyzed at 750 °C removed almost 100% of the Pb from a 5000 mg per L solution and had a maximum measured sorption capacity greater than 150 mg g^{-1} (Fig. 1 and Table 2). The sorption of Pb to these biochars made from plant materials may be attributed to the development of micropores due to the degradation of cellulose and hemicellulose.[26] Cellulose and hemicellulose degrade at a lower temperature than lignin, which is more prevalent in woody biochars and has been observed by Soria, Rolfe[27] to inhibit the sorption of Pb. The lower sorption in pine bark was therefore attributed to the decomposition of lignin blocking micropores and reducing the area of surface available for sorption. Cao, Shen[28] observed a maximum sorption capacity of wheat straw biochar pyrolyzed at 800 °C was 158 mg g^{-1}, similar to our findings that wheat straw biochar pyrolyzed at 750 °C had a Langmuir maximum sorption capacity (C_{sm}) of 164 mg g^{-1} (Table 2).

The Langmuir sorption isotherm model assumes that the adsorption process occurred through monolayer adsorption,[29] and so a good Langmuir fit provides some insights into the underlying mechanism, but not conclusive evidence of the sorption mechanisms. The sorption of Pb to biochars produced at low pyrolysis temperature could be attributed to specific adsorption (ion exchange) on oxygenated functional groups such as carboxyl groups and hydroxyl groups, which are prevalent on the surface of low pyrolysis temperature biochars.[17,21] The peaks observed in the FTIR spectra of biochars, when compared to their feedstocks, show that there is a loss of organic functional groups as the pyrolysis temperature increases (Fig. S-5†). The O–H bond stretch peak between 3500 cm^{-1} and 3200 cm^{-1} and the aliphatic C–H bond at approximately 2900 cm^{-1} to 2800 cm^{-1} were observed to show some resistance against degradation of cellulosic and ligneous components as pyrolysis temperature increased from 300 °C to 450 °C. Furthermore, peaks were observed between 1200 cm^{-1} and 1000 cm^{-1}, and between 900 cm^{-1} and 750 cm^{-1}, were attributed C–O and aromatic C–H, respectively (Table S-1†). The intensity of these peaks were steady between 300 °C to 400 °C, but diminished as the pyrolysis temperature increased above 400 °C which suggests the cracking and destruction of cellulose, hemicellulose and lignin structures. Our suggestion that oxygenated functional groups are responsible for Pb sorption to low temperature biochars is consistent with findings of Jiang, Yongbo,[30] Yan, Yu,[31] Yang, Sun,[32] and Soria, Rolfe[27] who all suggested that strong complexation with acidic functional groups were the mechanisms responsible for the sorption of metal cations to biochars pyrolyzed at low temperature.

Biochars pyrolyzed at high temperature contain fewer oxygenated functional groups on their surface (Fig. S-5†), as observed by Janu, Mrlik.[23] Therefore, the greater Pb sorption we observed with increasing pyrolysis temperature (Fig. 1) could not be attributed to formation of complexes with functional groups. The surface area and pore volume of biochars increases with an increase in the pyrolysis temperature[18] due to the breakdown of the recalcitrant C, creating more sorption sites on the biochar surface.[19] We observed FTIR peaks at 2158 cm^{-1} emerge in biochars pyrolyzed at temperatures of 600 °C and above (Fig. S-5†), indicative of vibrational overtones of aromatic C≡C structures (Table S-1†), and indicating greater aromaticity in biochars pyrolyzed at higher temperatures. The aromatic groups which become present on the surface of biochars produced at higher pyrolysis temperatures (≥600 °C) could be

responsible for the sorption of Pb through non-specific physical sorption due to cation–π interactions.[8] Wang, Gao[21] suggested that an interaction between Pb and π electrons occurred due to aromatic groups functioning as an electron donor as the aromaticity of biochar increased at higher pyrolysis temperatures (≥500 °C). Furthermore, Soria, Rolfe[27] also attributed Pb sorption to cation–π bonding and a pool of π electrons present in the aromatic structures at high pyrolysis temperature. Our observations therefore suggest that the greater sorption of Pb occurring on the surface of biochars produced at high pyrolysis temperature, compared to low pyrolysis temperature, is likely due to greater cation–π interactions with aromatic groups which were more abundant on the biochars at higher pyrolysis temperatures.

The maximum possible Pb sorption was significantly positively correlated with the feedstock N content (Fig. 2). Several studies have shown that a relationship exists between biochar feedstock elemental composition and the maximum sorption capacity. A relationship between the feedstock C/N ratio and the biochar Zn and Cu sorption capacity was reported by Rodríguez-Vila, Selwyn-Smith.[24] In another study, Ahmad, Gao[15] attributed the high N content in cauliflower biochar as being responsible for greater sorption capacity of Pb, Cu and Cd. Yu, Lian[33] showed that graphite-N on the surface of biochar was responsible for sorption of Cu and Cd *via* cation–π bonding in aqueous solution. These observations are in agreement with the assertion of Leng, Xu,[34] who attributed the greater sorption of heavy metals on N-doped biochars to the presence of N functional groups such pyrrolic-N, pyridinic-N, and graphite-N. Similarly, Jiang, Yang[35] revealed that corn straw biochars doped with urea to produce 3 sets of biochars specifically rich in pyrrolic-N, pyridinic-N, and graphite-N were able to adsorb more Cd from solution compared to pristine biochars. The highest Cd sorption occurred for graphite-N doped biochar due to its ability to form cation–π interactions with Cd from two adsorption sites. In another study, Lin, Yang[36] attributed the increase in the sorption of Cd and As to N doped biochar to the formation of porous structures and development of N-functional groups which can complex with heavy metals by sharing spare electrons.

The N content in the N-rich feedstocks (Table 1) used in our study may have lead to more heterocyclic N groups on the surface of the biochar[37] such as pyridine, pyrimidine, pyrrole, or imidazole, or polycyclic heterocycles such as indole, quinoline, isoquinoline, or purine. Due to N atoms being more electronegative than C atoms, biochars with more heterocyclic N are more likely to have greater π-electron density and act as an electron donor than biochars with less heterocyclic N (Fig. 3). A previous study by Lin, Yang[36] reported that quaternary-N increased the π-electron density of the biochar which enhanced the interaction of the π-donor with heavy metal ions. Therefore, the presence of heterocyclic N functional groups are one possible reason for the increased removal of Pb from solution by the biochars produced at high pyrolysis temperatures from feedstocks with high inherent N content,[34] and this requires further investigation. Nevertheless, regardless of the mechanism of sorption, our findings support the use of high nitrogen feedstocks for making biochars or doping feedstocks with nitrogen for maximum Pb sorption capacity.

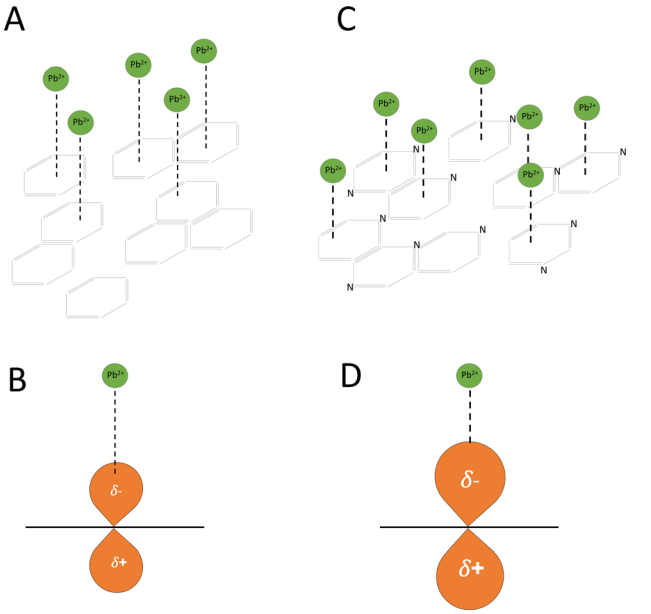

Fig. 3 Possible mechanism of Pb sorption biochars made from low N feedstocks (A and B) and high N feedstocks (C and D). (A and B) Represent a biochar with low N content pyrolyzed at high temperature resulting in cation–π interactions between aromatic groups on the biochar surface and Pb ions in solution. (C and D) Represent a biochar with high N content pyrolyzed at high temperature resulting in heterocyclic N structures which have a higher electron density and stronger cation–π interactions between heterocyclic N structures on the biochar surface and Pb ions in solution.

The findings reported in this paper advance our ability to maximize the efficiency of biochar production for the remediation of Pb contaminated soils and solutions. Currently, biochars are made from available feedstocks without full knowledge of what the resultant biochar properties will be and how effective the biochar will be for performing a specific function (*e.g.*, contaminant immobilization). The utility of other available feedstocks is unknown without arbitrary experimentation. This research provides a framework for an approach to address these uncertainties and inefficiencies that restrict the potential benefits of biochar production for end users. We report a formula that enables end users to select feedstocks that are optimal for Pb sorption based on the nitrogen content of the feedstock and suggest a possible mechanistic basis for the relationship.

Conclusion

We found that biochars made from four different feedstocks at 10 different pyrolysis temperatures could effectively remove Pb from aqueous solution to a varying extent. We observed a clear relationship of increasing sorption with increasing pyrolysis temperature, alongside a decrease in the abundance of oxygenated functional groups and greater aromaticity. We found a significant positive relationship between feedstock N

content and the maximum possible Pb sorption capacity at optimum pyrolysis temperature. One possible reason for this relationship is because biochars made from feedstocks that contain more N led to more heterocyclic N groups (*e.g.* pyridine, pyrimidine, pyrrole, or imidazole) or polycyclic heterocycles (*e.g.* indole, quinoline, isoquinoline, or purine) in the resulting biochar. These biochars may therefore be more electronegative and have greater π-electron density, which enhances cation–π interactions with Pb. However, this mechanism requires further work to confirm its prevalence and importance. More importantly, the quantification of this relationship between Pb sorption capacity and biochar feedstock N content enables us to predict the sorption capacity of biochars prior to pyrolysis by measuring or estimating their N content. Thus, remediation engineers can select feedstocks that optimise the production of cost effective biochars for contaminant remediation without the need for arbitrary experimentation.

Data availability

Data for this paper is freely available online: Ogbuagu Chinonso, Robinson Steve and Sizmur Tom, Data for: Feedstock nitrogen content mediates maximum possible Pb sorption capacity of biochars, Mendeley Data, V1, 2023, **https://doi.org/10.17632/g86tgcy22j.1**.

Author contributions

Chinonso Ogbuagu: data curation, formal analysis, funding acquisition, investigation, visualisation, writing – original draft. Steve Robinson: supervision, writing – review and editing. Tom Sizmur: conceptualization, resources, formal analysis, methodology, project administration, writing – review and editing.

Conflicts of interest

There are no conflicts to declare.

Acknowledgements

The authors wish to thank technical staff within the Department of Geography and Environmental Science, with special thanks to Anne Dudley, Karen Gutteridge, Sean Coole, Chris Speed, Fengjuan Xiao, and Elisa Alonso Lopez for their assistance with laboratory analysis.

References

1 R. Zhang, V. L. Wilson, A. Hou and G. Meng, Source of lead pollution, its influence on public health and the countermeasures, *Int. J. Health Animal Sci. Food Saf.*, 2015, **2**(1), 18–31.
2 J. Markus and A. B. McBratney, A review of the contamination of soil with lead: II. Spatial distribution and risk assessment of soil lead, *Environ. Int.*, 2001, **27**(5), 399–411.
3 L.-S. Zeng, M. Liao, C.-L. Chen and C.-Y. Huang, Effects of lead contamination on soil microbial activity and rice physiological indices in soil–Pb–rice (Oryza sativa L.) system, *Chemosphere*, 2006, **65**(4), 567–574.
4 M. A. Assi, M. N. M. Hezmee, M. Y. M. Sabri and M. A. Rajion, The detrimental effects of lead on human and animal health, *Vet. World*, 2016, **9**(6), 660.
5 B. Kavitha, P. V. L. Reddy, B. Kim, S. S. Lee, S. K. Pandey and K.-H. Kim, Benefits and limitations of biochar amendment in agricultural soils: a review, *J. Environ. Manag.*, 2018, **227**, 146–154.
6 J. Lehmann, Terra preta Nova–where to from here?, *Amazonian Dark Earths: Wim Sombroek's Vision*, Springer, 2009, pp. 473–486.
7 K. Komnitsas, D. Zaharaki, I. Pyliotis, D. Vamvuka and G. Bartzas, Assessment of pistachio shell biochar quality and its potential for adsorption of heavy metals, *Waste Biomass Valorization*, 2015, **6**(5), 805–816.
8 T. Sizmur, R. Quilliam, A. P. Puga, E. Moreno-Jiménez, L. Beesley and J. L. Gomez-Eyles, Application of biochar for soil remediation. *Agricultural and environmental applications of biochar: Advances and barriers*, 2016, vol. 63, pp. 295–324.
9 I. N. Anyanwu, M. N. Alo, A. M. Onyekwere, J. D. Crosse, O. Nworie, C. U. Uwa, *et al.*, Data on heavy metals content and biochar toxicity in a pristine tropical agricultural soil, *Data Brief*, 2018, **18**, 1064–1068.
10 P. Lucchini, R. Quilliam, T. H. DeLuca, T. Vamerali and D. L. Jones, Does biochar application alter heavy metal dynamics in agricultural soil?, *Agric., Ecosyst. Environ.*, 2014, **184**, 149–157.
11 S. Meyer, B. Glaser and P. Quicker, Technical, economical, and climate-related aspects of biochar production technologies: a literature review, *Environ. Sci. Technol.*, 2011, **45**(22), 9473–9483.
12 K. Homagain, C. Shahi, N. Luckai and M. Sharma, Life cycle cost and economic assessment of biochar-based bioenergy production and biochar land application in Northwestern Ontario, Canada, *For. Ecosyst.*, 2016, **3**(1), 1–10.
13 W. Gwenzi, N. Chaukura, C. Noubactep and F. N. Mukome, Biochar-based water treatment systems as a potential low-cost and sustainable technology for clean water provision, *J. Environ. Manag.*, 2017, **197**, 732–749.
14 H. Lu, W. Zhang, Y. Yang, X. Huang, S. Wang and R. Qiu, Relative distribution of Pb2+ sorption mechanisms by sludge-derived biochar, *Water Res.*, 2012, **46**(3), 854–862.
15 Z. Ahmad, B. Gao, A. Mosa, H. Yu, X. Yin, A. Bashir, *et al.*, Removal of Cu (II), Cd (II) and Pb (II) ions from aqueous solutions by biochars derived from potassium-rich biomass, *J. Clean. Prod.*, 2018, **180**, 437–449.
16 L. Liu, Y. Huang, Y. Meng, J. Cao, H. Hu, Y. Su, *et al.*, Investigating the adsorption behavior and quantitative contribution of Pb2+ adsorption mechanisms on biochars by different feedstocks from a fluidized bed pyrolysis system, *Environ. Res.*, 2020, **187**, 109609.
17 L. Gao, Z. Li, W. Yi, Y. Li, P. Zhang, A. Zhang, *et al.*, Impacts of pyrolysis temperature on lead adsorption by cotton stalk-

derived biochar and related mechanisms, *J. Environ. Chem. Eng.*, 2021, **9**(4), 105602.

18 K. Jindo, H. Mizumoto, Y. Sawada, M. Sanchez-Monedero and T. Sonoki, Physical and chemical characterizations of biochars derived from different agricultural residues, *Biogeosci. Discuss.*, 2014, **11**(8), 11727–11746.

19 A. Tomczyk, Z. Sokołowska and P. Boguta, Biochar physicochemical properties: pyrolysis temperature and feedstock kind effects, *Rev. Environ. Sci. Bio/Technol.*, 2020, **19**(1), 191–215.

20 C. Figueiredo, H. Lopes, T. Coser, A. Vale, J. Busato, N. Aguiar, *et al.*, Influence of pyrolysis temperature on chemical and physical properties of biochar from sewage sludge, *Arch. Agron Soil Sci.*, 2018, **64**(6), 881–889.

21 S. Wang, B. Gao, A. R. Zimmerman, Y. Li, L. Ma, W. G. Harris, *et al.*, Physicochemical and sorptive properties of biochars derived from woody and herbaceous biomass, *Chemosphere*, 2015, **134**, 257–262.

22 W. Ding, X. Dong, I. M. Ime, B. Gao and L. Q. Ma, Pyrolytic temperatures impact lead sorption mechanisms by bagasse biochars, *Chemosphere*, 2014, **105**, 68–74.

23 R. Janu, V. Mrlik, D. Ribitsch, J. Hofman, P. Sedláček, L. Bielská, *et al.*, Biochar surface functional groups as affected by biomass feedstock, biochar composition and pyrolysis temperature, *Carbon Resour. Convers.*, 2021, **4**, 36–46.

24 A. Rodríguez-Vila, H. Selwyn-Smith, L. Enunwa, I. Smail, E. F. Covelo and T. Sizmur, Predicting Cu and Zn sorption capacity of biochar from feedstock C/N ratio and pyrolysis temperature, *Environ. Sci. Pollut. Res.*, 2018, **25**(8), 7730–7739.

25 C. Ogbuagu, S. Robinson, T. Sizmur, *Data for: Feedstock nitrogen content mediates maximum possible Pb sorption capacity of biochars*, Mendeley Data, 2023, DOI: **10.17632/g86tgcy22j.1**.

26 M. Askeland, B. Clarke and J. Paz-Ferreiro, Comparative characterization of biochars produced at three selected pyrolysis temperatures from common woody and herbaceous waste streams, *PeerJ*, 2019, **7**, e6784.

27 R. I. Soria, S. A. Rolfe, M. P. Betancourth and S. F. Thornton, The relationship between properties of plant-based biochars and sorption of Cd (II), Pb (II) and Zn (II) in soil model systems, *Heliyon*, 2020, **6**(11), e05388.

28 Y. Cao, G. Shen, Y. Zhang, C. Gao, Y. Li, P. Zhang, *et al.*, Impacts of carbonization temperature on the Pb (II) adsorption by wheat straw-derived biochar and related mechanism, *Sci. Total Environ.*, 2019, **692**, 479–489.

29 The Langmuir isotherm adsorption equation: the monolayer approach, *IOP Conference Series: Materials Science and Engineering*, ed. E. Heraldy, Y. Hidayat and M. Firdaus, IOP Publishing, 2016.

30 J. Jiang, P. Yongbo, Y. Min, H. Zhineng, W. Dejian and X. Renkou, Rice straw-derived biochar properties and functions as Cu (II) and cyromazine sorbents as influenced by pyrolysis temperature, *Pedosphere*, 2015, **25**(5), 781–789.

31 S. Yan, W. Yu, T. Yang, Q. Li and J. Guo, The Adsorption of Corn Stalk Biochar for Pb and Cd: Preparation, Characterization, and Batch Adsorption Study, *Separations*, 2022, **9**(2), 22.

32 Y. Yang, F. Sun, J. Li, J. Chen and M. Tang, The effects of different factors on the removal mechanism of Pb (ii) by biochar-supported carbon nanotube composites, *RSC Adv.*, 2020, **10**(10), 5988–5995.

33 W. Yu, F. Lian, G. Cui and Z. Liu, N-doping effectively enhances the adsorption capacity of biochar for heavy metal ions from aqueous solution, *Chemosphere*, 2018, **193**, 8–16.

34 L. Leng, S. Xu, R. Liu, T. Yu, X. Zhuo, S. Leng, *et al.*, Nitrogen containing functional groups of biochar: an overview, *Bioresour. Technol.*, 2020, **298**, 122286.

35 Y. Jiang, C. Yang, Q. Yao, Y. Deng, J. Yang, Y. Liu, *et al.*, Contribution of nitrogen configurations to the adsorption of Cd (ii) in nitrogen-enriched biochar, *New J. Chem.*, 2021, **45**(28), 12669–12677.

36 S. Lin, X. Yang, L. Liu, A. Li and G. Qiu, Electrosorption of cadmium and arsenic from wastewaters using nitrogen-doped biochar: mechanism and application, *J. Environ. Manage.*, 2022, **301**, 113921.

37 W. Chen, K. Li, M. Xia, Y. Chen, H. Yang, Z. Chen, *et al.*, Influence of NH3 concentration on biomass nitrogen-enriched pyrolysis, *Bioresour. Technol.*, 2018, **263**, 350–357.